

# A CONCEPTUAL MODELING OF ULTRASONIC TOMOGRAPHY SYSTEM TO DETECT EARLY CARIES LESIONS

Nurul I'zaaz Mohd Zulkifli<sup>a</sup>, Juliza Jamaludin<sup>a\*</sup>, Normaliza Ab Malik<sup>b</sup>, Farah Aina Jamal<sup>c</sup>, Nik Halimatun Sadiyah Nik Abdul Razak<sup>a</sup>

<sup>a</sup>Faculty of Engineering and Built Environment, Universiti Sains Islam Malaysia, 71800 Nilai, Negeri Sembilan, Malaysia

<sup>b</sup>Faculty of Dentistry, Universiti Sains Islam Malaysia, 71800 Nilai, Negeri Sembilan, Malaysia

<sup>c</sup>Faculty of Electrical Engineering, Universiti Teknologi Malaysia, 81310 UTM Johor Bahru, Johor, Malaysia

## Article history

Received

14 August 2023

Received in revised form

22 October 2023

Accepted

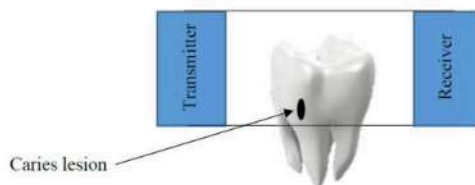
25 November 2023

Published Online

20 April 2024

\*Corresponding author  
juliza@usim.edu.m

## Graphical abstract



## Abstract

Dental diagnostic imaging plays a significant role in the field of dentistry. In the oral environment, continuous demineralization and remineralization of tooth structure is common. Early diagnosis and monitoring of carious lesions are essential, and enamel abnormalities require quantitative imaging techniques. Among the imaging modalities available are radiography, X-ray computed tomography, and magnetic resonance imaging. However, to obtain imaging information on dental diagnostics, most of these systems rely on specific radiation and energy which might be harmful to health. To overcome the aforementioned problem, this research proposes a conceptual modeling of ultrasonic tomography system to detect enamel abnormalities using simulation from COMSOL software. Ultrasonic tomography can be obtained by the presence of acoustic waves transmitted from a source and the reflection of the waves at the investigated area. The transmission technique yielded 0.0041260 V for 7 MHz and 0.0003841 V for 25 MHz, but the reflection method yielded 0.000060 V for 7 MHz and 0.000211 V for 25 MHz. The transmission approach produces the greatest difference in voltage when compared to the reflection method. This suggests that, in comparison to the reflection technique, the transmission method is significantly better at detecting changes on the tooth surface.

**Keywords:** Ultrasonic tomography, dentistry, caries lesion, transmission method, imaging

## Abstrak

Pengimejan diagnostik pergigian memainkan peranan penting dalam bidang pergigian. Persekitaran mulut, demineralisasi dan remineralisasi berterusan pada struktur gigi adalah perkara yang biasa berlaku. Diagnosis dan pemantauan awal pembentukan karies gigi adalah penting dan memertukan teknik pengimejan kuantitatif. Antara kaedah pengimejan yang sediaada ialah radiografi, tomografi berkomputer sinar-X dan pengimejan resonan magnetik. Walaubagaimanapun, sistem maklumat pengimejan seperti diatas kebanyakannya bergantung kepada penggunaan radiasi pada skala kecil yang berbahaya kepada kesihatan jika pesakit kerap terdedah. Untuk mengatasi masalah yang disebutkan diatas, cadangan pemodelan konsep sistem tomografi ultrasonik untuk mengesan perubahan

enamel gigi menggunakan perisian COMSOL diperkenalkan. Tomografi ultrasonik adalah berdasarkan gelombang akustik yang dihantar secara terus dan hasil daripada pantulan gelombang tersebut di kawasan yang terlibat akan dianalisis. Tomografi ultrasonik yang menggunakan teknik langsung menghasilkan 0.0041260 V bagi nilai frekuensi 7 MHz dan 0.0003841 V bagi nilai frekuensi 25 MHz, manakala kaedah tomografi ultrasonik tidak langsung menghasilkan 0.000060 V bagi nilai frekuensi 7 MHz dan 0.000211 V bagi nilai frekuensi 25 MHz. Didapati tomografi ultrasonik yang menggunakan teknik langsung menghasilkan perbezaan voltan yang paling besar jika dibandingkan dengan teknik tidak langsung. Ini menunjukkan bahawa, tomografi ultrasonik yang menggunakan teknik langsung jauh lebih baik untuk mengesan perubahan pada permukaan gigi yang disebabkan oleh karies.

*Kata kunci:* Tomografi ultrasonik, pergigian, lesi karies, kaedah langsung, pengimejan

© 2024 Penerbit UTM Press. All rights reserved

## 1.0 INTRODUCTION

One of the strategies for creating a cross-sectional picture from data acquired by the system is to use a tomography system. The basic concept of tomography is to collect data from sensors positioned around targeted area to determine the distributions of items. In tomographic imaging, waves or radiation are used to study the structure and composition of objects and then to estimate virtual cross sections over them [1].

The initial sign of a new carious lesion is a chalky white spot on the tooth's surface, indicating an area of enamel demineralization. Quantitative imaging techniques are required for the early detection and monitoring of carious lesions and enamel anomalies. The existence of acoustic waves sent from a source and their reflection at the studied region may be determined via ultrasonic tomography.

The goal of the research is to create a conceptual model of ultrasonic tomography that may be used in dental diagnostic using COMSOL software simulation. The frequency of transmission and reception will be analyzed to discover any irregularities in the targeted location, allowing the detection of tooth anomalies.

The objectives of this research are: (i) to design the configuration conceptual modeling for ultrasonic tomography in the detection of teeth abnormalities, (ii) to conduct several simulations of the ultrasonic tomography and construct the image to be analyzed and (iii) to verify the capability of the ultrasonic tomography system to detect early caries lesion.

The appearance of a chalky white spot on the tooth's surface is the first indicator of a new carious lesion. This is caused by the demineralization or deterioration of the enamel. If left untreated, it develops into a cavity, and the enamel can no longer be repaired [2]. Quantitative imaging techniques are required for the early detection and monitoring of carious lesions and enamel anomalies.

There are several available intra-oral radiograph methods that are being used in the field of dentistry to identify any tooth abnormalities such as bitewing and periapical radiograph. However, these existing modalities are associated with a few difficulties and disadvantages. Furthermore, most of these systems may be harmful to human health due to the high level of radiation exposure,

In this research, the main and outermost layer (enamel) was used in the design process as at this stage COMSOL cannot be used for any other layers. In this case, only the upper front teeth (maxillary central incisor) was used in the research as the conceptual model for the system.

Unlike conventional computed axial tomography, in which X-ray photons travel parallel to one another, the X-ray beam in dental Cone Beam Computed Tomography (CBCT) has a characteristic cone or pyramidal form. The form of the main X-ray beam, as well as the complete arc travelled, may have an influence on caries diagnosis. If a machine merely spins 180° in an arc around the object of interest, a shadow zone will be created around it. The shadow zone is an area where there is a lack of radiography signal reaching the receptor, resulting in the creation of areas where no anatomic information is available to produce an image [3]. The CBCT method has limitations in that it may cause the image to be warped on the periphery; moreover, it requires the patient's head to remain still; hence, may cause discomforts to the patients. This technique may not be suitable for very young children, those unable to remain still, or those with movement problems [3]. The use of dental CBCT is also limited by the hazardous ionizing radiation it emits [4], which is the most significant drawback of computed tomography (CT) imaging [5].

Next, the existing modalities such as bitewing radiograph, requires patient to stabilizes the receptor by biting on a tab or bitewing holder. The central ray of the X-ray beam is then transmissioned through the contacts of the posterior teeth in occlusion. The

sensors, which are mounted above silicon crystal plates, are made from chips. When silicon crystals are subjected to radiation, they absorb energy and convert it to light. The quantity of light emitted is recorded by the sensor's chip. After exposure, the sensors can send visual data to a computer via wire or radio waves to a receiver connected to a computer [3]. Image analysis can induce bias on the side of the user, and the location of the image sensor in the mouth might result in retakes due to incorrect positioning. Furthermore, the harmful ionizing radiation of radiography limits the usage. In addition, bitewing radiograph may cause discomfort to patient because of its bulky tools such as film or digital receptors [6].

Optical Coherence Tomography (OCT) is a non-invasive technology that produces horizontal pictures of a tooth anatomy. In principle, it is an interferometric method that uses infrared light waves to reflect off the inner microstructure in a similar way to an ultrasonic pulse echo [7]. Typically, OCT systems have a resolution of 20–5  $\mu\text{m}$  [8]. The principle of the OCT system is illustrated in Figure 1. The swept sources (SS) emit a low-coherent light that passes through the beam splitter before splitting into two beams at the fiber coupler. A moving reference mirror arm receives one beam, whereas a sample arm receives the other. At the fiber coupler, the reference arm's back-reflected beam and the sample arm's backscattered beam are reunited and transported to a photo detector [9]. One limitation of OCT is the shallow penetration depth caused by signal attenuation due to scattering and absorption. OCT can image structures up to a depth of 2.5 mm [5]. Magnetic Resonance Imaging (MRI), a non-invasive technology, is used to identify internal structures, discriminate soft and hard tissues, and assess a number of physio-logical processes [10]. The hydrogen nucleus emits a resonance signal, which causes protons throughout the body to align with it by creating a strong magnetic field with strong magnets. The protons are activated and spin out of equilibrium when a radiofrequency current is pulsed through the patient. When the radiofrequency field is switched off, the MRI sensors can measure the energy generated when the protons realign with the magnetic field. The quantity of energy released and the time it takes for the protons to realign with the magnetic field vary depending on the environment and chemical makeup of the molecules. These magnetic properties allow doctors to distinguish between different types of tissues. A patient is put within a huge magnet to produce an MRI scan and must remain motionless during the imaging process to avoid blurring the image [11]. The drawbacks of MRI include its high cost and high noise level. It is also contraindicated in individuals with cardiac pacemakers, implanted defibrillators, and other devices that might cause claustrophobia [11].

X-ray CT shows an object's underlying structures by using a thin fan shaped X-ray beam and several exposures surrounding it, allowing the clinician to see

morphologic characteristics and pathologies in three dimensions. A CT scanner consists of a radiographic tube and a series of scintillation detectors, often known as ionization chambers. Within the gantry, the tube head and reciprocal detectors either spin synchronously around the patient, or the detectors create a continuous ring around the patient, with the X-ray tube moving in a circle within the ring. The high level of radiation exposure is the major disadvantage of CT imaging. Other disadvantages of CT include high scan prices and scatter generated by metallic objects. Compared with traditional radiography, it has a low resolution. CT has limitations in the identification of dental fractures (such as tiny fissures on the tooth surfaces) that are below the resolution capabilities of CT, which can lead to false negative results [12]. Table 1 summarized the methods and their limitations.

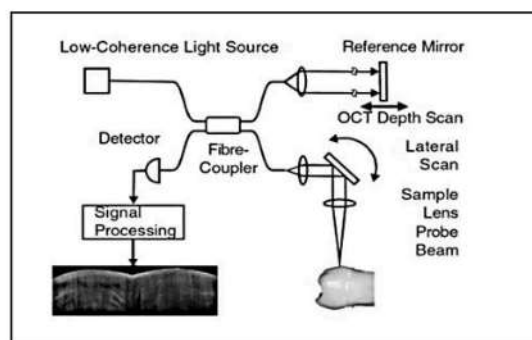


Figure 1 Principles of OCT [9].

Caries is normally diagnosed via X-rays, visual inspection, or a steel pick; however, Ultrasonography (USG) may be able to offer a far earlier diagnosis without ionizing radiation, even when the lesion is in a fragile state which can be remineralized rather than drilled and filled. Ultrasound with frequencies ranging from 3 to 12 MHz is commonly employed in dentistry [5]. Ultrasound is based on the reflection of sound waves with frequencies outside the range of human hearing (1–20 kHz) at the interface of tissues with different acoustic properties. The piezoelectric action within a transducer produces ultrasonic waves (probe). A transducer detects the echoes and turns them into an electrical signal, which is shown on a computer screen in real time in black, white, and shades of grey [12].

Compared with other prominent methods of medical imaging, USG has several advantages: it provides images in real time and is portable, inexpensive, radiation-free, non-invasive, and unaffected by metal artifacts, such as dental restorations [13]. The benefits of USG in dentistry include the ability to evaluate volume data in several imaging planes and precise assessment of lesion volume. Furthermore, it provides both disease diagnosis and image guidance for minimally invasive therapy. The relative cheap cost and ease of use of 3D ultrasound over existing intraoperative imaging

modalities are its main advantages, as well as its capacity to determine the length, area, and volume of organs or lesions in any orientation [14].

These are some of the limitations of ultrasonic tomography. The approach is very reliant on the operator and the equipment used. It must be carried out by qualified investigators [14]. For the proper interpretation of ultrasound images, a qualified radiologist with extensive experience in the use and interpretation of ultrasound images is essential [12]. Ultrasound images are impacted by inherent noise in the signal returned to the transducer, which makes it difficult to interpret static images and, in certain cases, dynamic images, and a non-moving object's appearance will change as a result of this noise [15] [16].

**Table 1** Methods and their limitations.

Methods	Limitations	References
Cone Beam Computed Tomography (CBCT)	1. Must remain still.	[4]
	2. Periphery image may be distorted.	
	3. Radiation exposure.	
Bitewing Radiograph	1. Produce image on user's bias.	[3]
	2. Error positioning.	
	3. Radiation exposure.	
Optical Coherence Tomography (OCT)	1. Shallow penetration depth.	[9]
	2. Signal attenuation and scattering.	
Magnetic Resonance Imaging (MRI)	1. Remain very motionless.	[11]
	2. expensive and very noisy.	
	3. Claustrophobia.	
	4. Contraindicated in patients with cardiac pacemakers, implantable defibrillators etc.	
X-Ray Computed Tomography	1. Radiation exposure.	[12]
	2. High cost.	
	3. Scatter because of metallic objects.	
	4. Limitation in the diagnosis of dental fractures and may result in false-negative readings.	

## 2.0 MATERIALS AND METHODS

Figure 2 below shows the flowchart of a conceptual modeling of ultrasonic tomography system to detect early caries lesions. To achieve the objective of the research, the configuration conceptual modeling

was designed using the COMSOL software. Next, multiple ultrasonic tomography simulations were conducted, and the image to be evaluated was generated to confirm the ultrasonic tomography system's capacity to detect early caries lesions.

The cross-sectional geometry of an ultrasonic piezoelectric MEMS device was created and simulated as transmitter and receiver using this model. The parameters were developed and examined using the documentation of the piezo acoustic transducer model in COMSOL Multiphysics 5.6a [17]. The lead zirconate titanate ( $\text{Pb}[\text{Zr}_{x}\text{Ti}_{1-x}]\text{O}_3$ ), often known as PZT ceramics, has become the dominating material in the ultrasonic transducer business. Tao Li *et al.* fabricated a tiny piezoelectric ultrasonic transducer based on PZT [18]. A pulse of electric signal excites the first transducer, which is coupled to an electric circuit. The other transducers are used as signal receivers and are affixed to the opposite side of the tooth.

Several experiments were conducted accordingly to determine the most suitable characteristics of the proposed system. From the experiments, the result of the simulation for each design was observed. Then, the difference in value at the probe was identified. The experiment was conducted to verify or refute a hypothesis, as well as to test the efficacy or probability of something that had never been done before. These experiments indicate what occurs when a specific component is altered, revealing cause and effect correlations. First and foremost, a 2D space dimension was selected, and then the physics interface was added that was used for the ultrasonic system, solid mechanics, electrical circuit, pressure acoustics, and electrostatic.

Acoustics of pressure, the pressure fluctuations for the propagation of acoustic waves in fluids at quiescent background conditions are computed using transient. It is suitable for all frequency-domain pressure field simulations with harmonic fluctuations (unit pascal (Pa)). The solid mechanics interface is built on solving the equations of motion in conjunction with a solid material constitutive model. The enamel substance, which is calcium HA, is used as the solid material in this situation. Electrostatic function is used to compute the electric field, electric displacement field, and potential distributions in dielectrics in electrostatics when the electric charge distribution is clearly established. Electrical circuits include voltage and current sources, resistors, capacitors, inductors, and semiconductor devices and are used to display the currents and voltages in circuits. Linkages to distributed field models may be found in electrical circuit interface models. The capacity of some materials to create an electric charge in response to applied mechanical stress is known as the piezoelectric effect. When a piezoelectric material is subjected to mechanical stress, the positive and negative charge centers change in the material, resulting in an external electrical field. When reversed, an outside electrical field either stretches or compresses the piezoelectric

material [19]. The most common piezoelectric material in use is PZT, which is a lead-based piezoelectric ceramic. PZT ceramics have been widely used for a sensor owing to its strong piezoelectric property; piezoelectricity is the process of using crystals to convert mechanical energy into electrical energy [19]. In this model, PZT-5H is used as the material for transmitter and receiver.

To explore the difference value of sensor voltage value, a specific component of the system is modified, as well as the value of the frequency that will be injected. Another thing that has changed is the state of the materials used in each design. The condition is set where there is a design with a normal condition where the material is merely enamel and a condition with anomalies where the enamel with the presence of air indicates an obstacle to teeth. Furthermore, the frequency value is altered to track changes in the system's simulation results, with the goal of determining the best frequency for use in ultrasonic tomography for early caries detection. Table 2 presents the summarize of the simulation testing conducted for two different frequency values, which are 7 and 25 MHz, while having different conditions of material. In (a), the material is enamel only; in (b), there are enamel and air material; and in (c), there are enamel material and air with anomalies having different sizes and positions.

**Table 2** Simulation testing with modified component

Frequency – 7MHz	Frequency – 25MHz
	(a) Enamel
	(b) Enamel + Air
	(c) Enamel + Air (different size and position)

### 3.0 RESULTS AND DISCUSSION

Figure 3 presents the set of model in a 2D axisymmetric configuration, which contains the transmitter, receiver, and material (enamel). The transmitter and receiver both have 0.5mm width and 0.5mm height. The enamel material is modeled according to the average of the actual measurement of the teeth and enamel, where the thickness of the enamel in the upper front teeth (maxillary incisor) is 1.5mm and the width of the teeth is 9.5mm. The transmitter and receiver are placed separately.

The transmitter is driven to send out a pulsed wave. The ultrasonic model uses a transducer to send out an acoustic pulse that travels through the material at a velocity that related to the lithology and porosity of the materials. The receivers may detect the signals of acoustic energy that travels through the material and reaches the receiver. The receiver converts the mechanical signal to an electrical signal, and the transmission times between the transmitter and receiver was recorded for velocity logging.

Figure 4 and 5 presents the position or arrangement of the transmitter and receiver for both the reflection and transmission methods. The blue line in the figure indicates the selected area as transmitter, and the red line indicates the sensor/receiver placement for transmitter. In COMSOL, the selected area were determined by the boundary probe and global variable probe. A specific component of the system, as well as the value of the frequency that will be injected, are changed to investigate the difference. Aside from that, the status of the materials used in each design has altered. The high and lower frequencies were used to inject at each design. These frequencies values were chosen from the previous research on the ultrasound in dentistry. The previous study from Wang, Hsiao-Chuan; Fleming, Simon; Lee, Yung-Chun; Swain, Michael; Law, Susan; Xue, Jing (2011). Laser ultrasonic evaluation of human dental enamel during remineralization treatment conduct an experiment for laser ultrasonic in human tooth. It stated that the level of mineralization of dental enamel is closely linked to its stiffness and/or elastic response. In the current study, the usable frequency bandwidth of the generated Surface Acoustic Wave that they investigated was between 7 ~ 25 MHz [20].

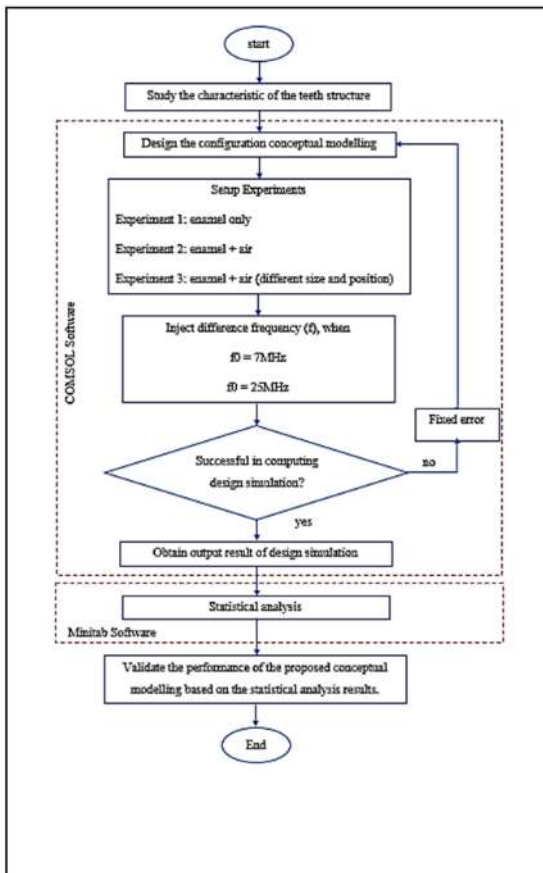


**Figure 2** The flowchart of a conceptual modeling of ultrasonic tomography system to detect early caries lesions

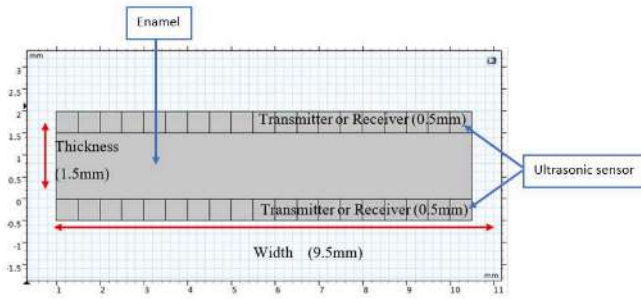


Figure 3 Top view of geometry design for central incisor with transmitter and receiver

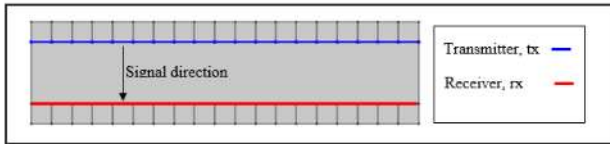


Figure 4 The transmitter and receiver position for Reflection method

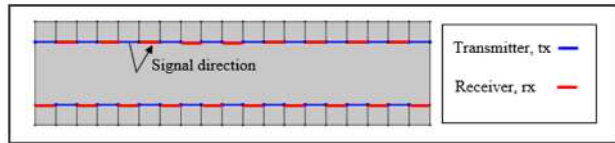


Figure 5 The transmitter and receiver position for Transmission method

For the first simulation, the material is set to be enamel or calcium hydroxyapatite in which, the initial frequency,  $f_0$  was injected with 7 MHz. For the second simulation, the material was also set to be enamel or calcium hydroxyapatite in which the initial frequency,  $f_0$  was injected with 25 MHz. The simulation results were presented as in Table 3. Each simulation for two different frequencies were carried out using two methods: reflection and transmission.

There was a difference in the image on wave propagation for the 7- and 25-MHz frequencies. For the 7-MHz frequency, the wave has a bigger propagation pattern, whereas for the 25-MHz frequency, there was a much smaller propagation wave pattern. Furthermore, the pixel value for the reflection method of 7 MHz ranges from 60 to -60; for the reflection method of 25 MHz, it ranges from 100 to -100; for the transmission method of 7 MHz, it ranges from 100 to -100; and lastly, for the transmission method of 25 MHz, it ranges from 150 to -150.

Figure 6 and 7 presents the scatter plot graph when simulating two difference frequencies for the reflection method. The difference that can be shown from the simulation was that the maximum voltage in the 7-MHz simulation is 0.15049 V, whereas the maximum voltage in the 25MHz simulation is 0.026944 V. The lower frequency, which was 7 MHz, has a higher voltage value than 25 MHz. The result from the simulation for the enamel only material was used to

identify the difference in voltage in the difference frequencies for the transmission method.

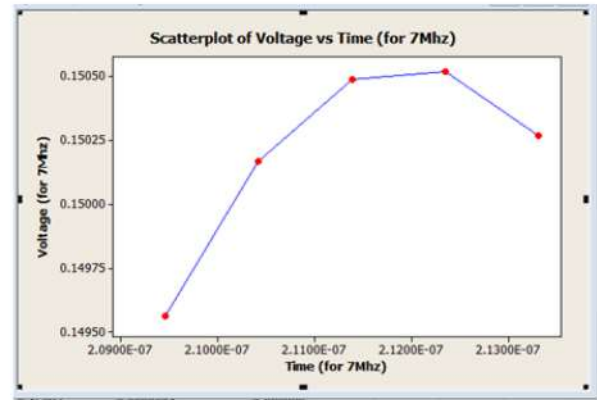


Figure 6 Scatter plot for 7 MHz – reflection

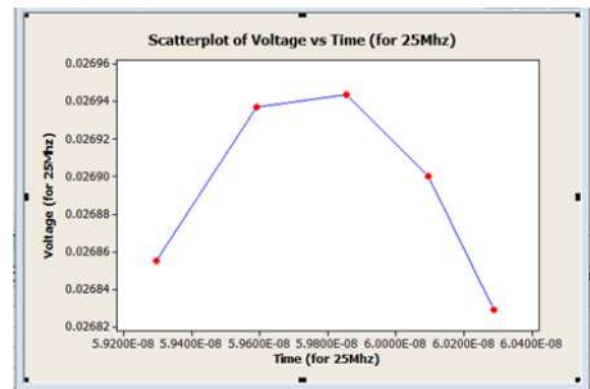


Figure 7 Scatter plot for 25 MHz – reflection

Figure 8 and 9 presents the scatter plot graph when simulating two difference frequencies for the transmission method. The difference that can be shown from the simulation was that the maximum voltage in the 7-MHz simulation is 0.058648 V, whereas the maximum voltage in the 25-MHz simulation is 0.0018895 V. The lower frequency, which was 7 MHz, has a higher voltage value than 25 MHz. For the next simulation, the material was set to be enamel or calcium HA with the presence of air gap to indicate the tooth problem, and the initial frequency,  $f_0$ , is injected with 7 MHz. Under the same condition,  $f_0$  is injected with 25 MHz. The simulation results are presented Table 4. The black dot indicates the small air gap (0.25 mm); red dot, the bigger air gap (0.7 mm); and the green dot, the position of the air gap. For each simulation in two difference frequencies are done in two methods which are reflection method and transmission method.

Figure 10 and 11 presents the scatter plot graph when simulating two difference frequencies for the reflection method. The difference that can be shown from the simulation is that the maximum voltage in the 7-MHz simulation is 0.15043 V, whereas the maximum voltage in the 25-MHz simulation is 0.026773 V. The lower frequency, which is 7 MHz, has a higher

voltage value than 25 MHz. Figure 12 and 13 present the scatter plot graph when simulating two difference frequencies for the transmission method. The difference that can be shown from the simulation is that the maximum voltage in the 7-MHz simulation is 0.054522 V, whereas the maximum voltage in the 25-MHz simulation is 0.0015054 V. The lower frequency, which is 7 MHz, has a higher voltage value than 25 Mhz.

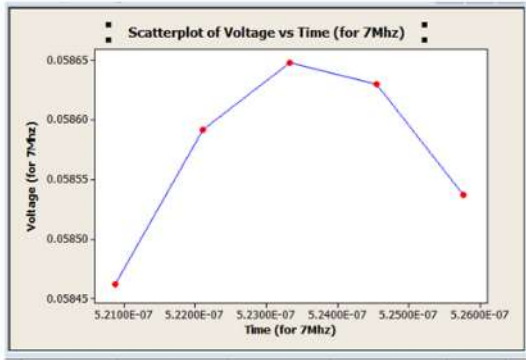


Figure 8 Scatter plot for 7 MHz – transmission

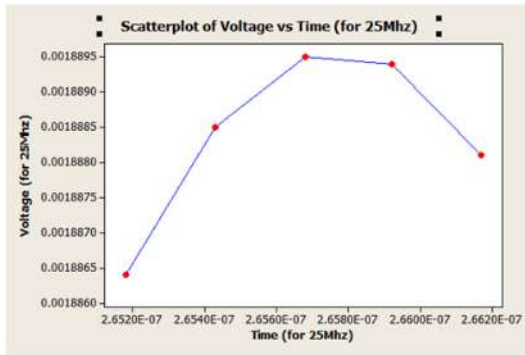


Figure 9 Scatter plot for 25 MHz – transmission

For the next simulation, the material was set to be enamel or calcium HA with the presence of air gap but with different sizes and positions. The initial frequency,  $f_0$ , is injected with 7 MHz, and then, under the same condition,  $f_0$  is injected with 25 MHz for the next simulation. The simulation results are presented in Table 5. For each simulation in two difference frequencies are done in two methods which are the reflection and transmission methods.

The result from the simulation for the enamel material with the presence of air gap at different sizes and positions is used to identify the difference in voltage of difference frequencies for the reflection method. This scatter plot has been plot based on receiver's voltage and time, whereas, ( $V_s \cdot T_s$  is plot for

smaller air gap), ( $V_b \cdot T_b$  is plot for bigger airgap) and ( $V_p \cdot T_p$  is plot for the different position air gap).

Table 3 Simulation of enamel material

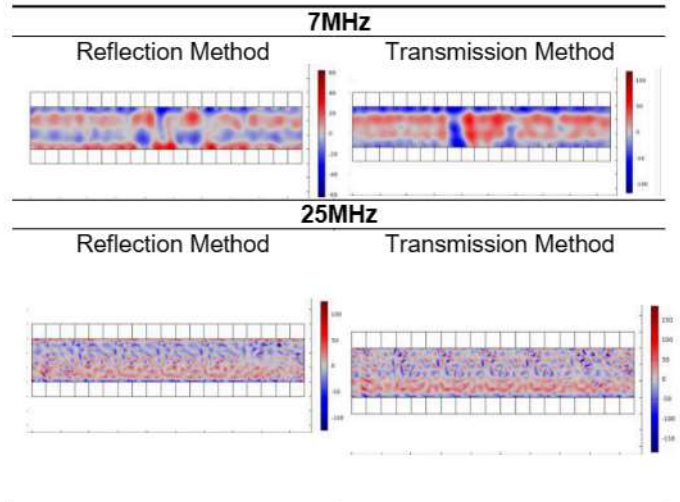


Table 4 Simulation of enamel with the presence of air gap

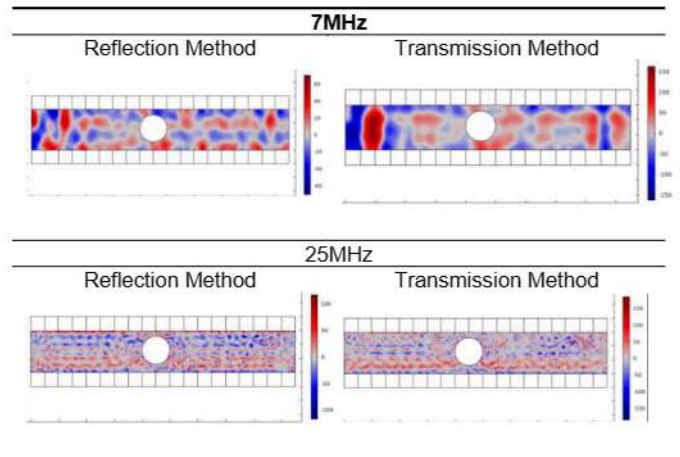


Figure 14 and 15 presents the scatter plot graph when simulating two difference frequencies for the reflection method and when three different states of the tooth are applied. Based on the scatter plot for both frequency values, the air gap with a bigger diameter (0.7 mm) results in a much lower voltage than the other two states.

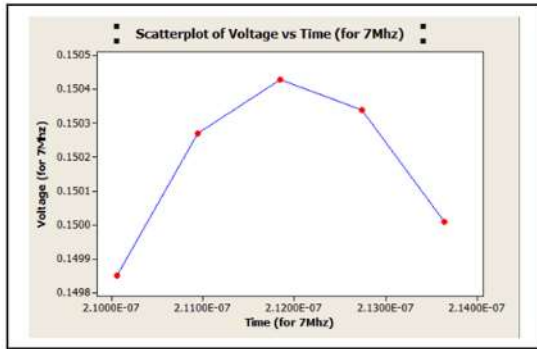


Figure 10 Scatter plot for 7 MHz – reflection

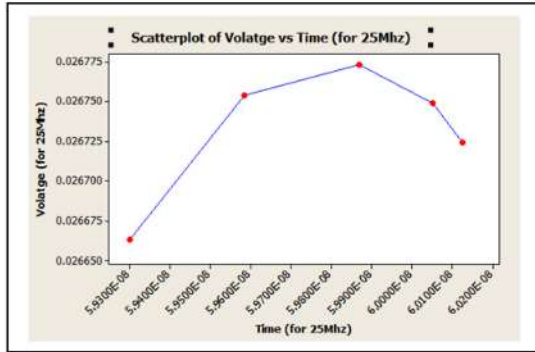


Figure 11 Scatter plot for 25 MHz – reflection

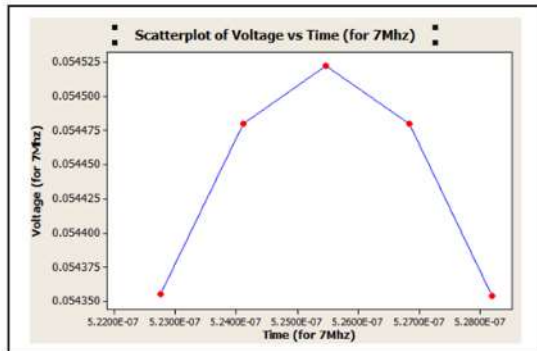


Figure 12 Scatter plot for 7 MHz – transmission

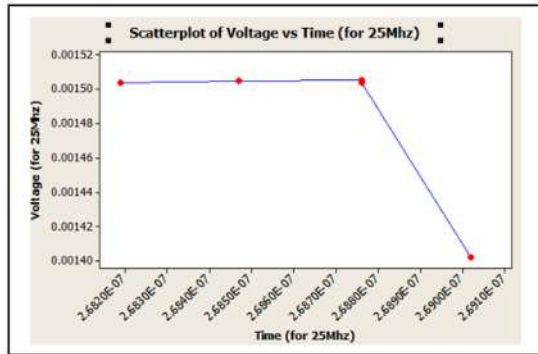


Figure 13 Scatter plot for 25 MHz – transmission

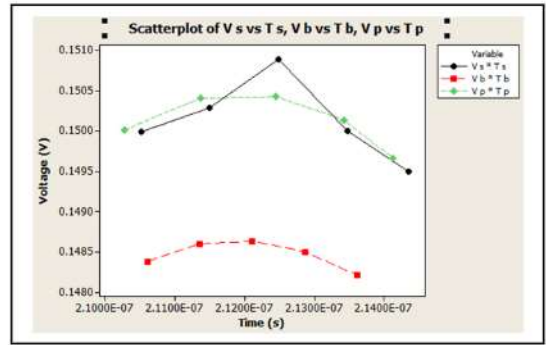


Figure 14 Scatter plot for 7 MHz with three different states of the tooth – reflection

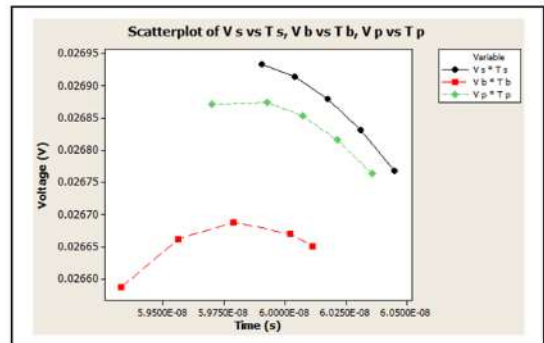


Figure 15 Scatter plot for 25 MHz with three different states of the tooth – reflection

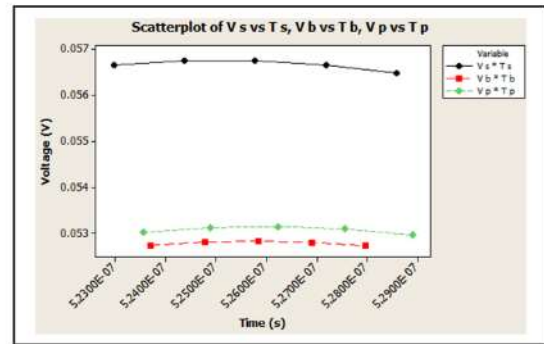


Figure 16 Scatter plot for 7 MHz with three different states of the tooth – transmission

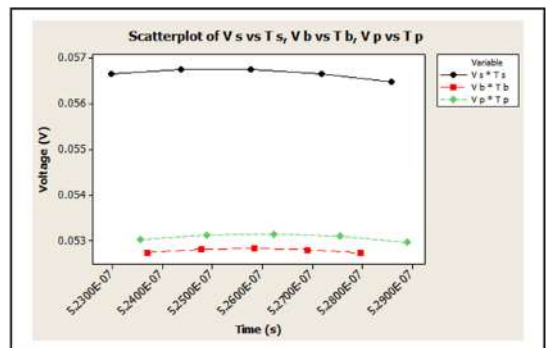


Figure 17 Scatter plot for 25 MHz with three different states of the tooth – transmission

**Table 5** Simulation of enamel with the presence of air gap with different sizes and positions

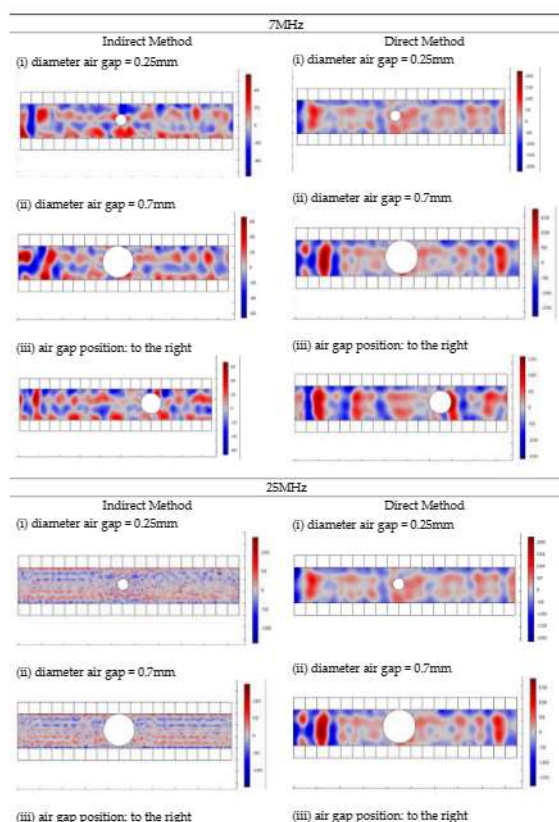


Figure 16 and 17 presents the scatter plot graph when simulating two different frequencies for the reflection method and when three different states of the tooth are applied. The black dot indicates the small air gap (0.25 mm); red dot, the bigger air gap (0.7 mm); and the green dot, the position of the air gap. Based on the scatter plot for both frequency values, the air gap with bigger diameter (0.7 mm) in the transmission method also results in a much lower voltage than the other two states.

Furthermore, the simulations for three states (when enamel with presence of air gap at different position and size) yielded varied results, indicating that the system is capable of detecting and identifying dental irregularities. Furthermore, Pulser-receivers (also known as pulser/receivers) produce ultrasonic pulses that are transmitted through materials for non-destructive testing (NDT). When the pulser's trigger is triggered, it creates brief, big amplitude electrical pulses (pulse voltage).

High frequency produces shorter wavelength, whereas low frequency produces longer wavelength; the use of shorter wavelengths improves resolution. To generate a shorter wavelength, a high frequency is used [21]. In Table 6, the difference in the voltage values for the two different methods can be clearly seen when the receiver voltage (enamel only) is subtracted from the receiver voltage (EA gap), produce the difference in sensor voltage loss.

The transmission method yielded 0.0041260 V for 7 MHz and 0.0003841 V for 25 MHz, but the reflection method yielded 0.000060 V for 7 MHz and 0.000211 V for 25 MHz, as presented in the table. In this situation, the transmission method produces the greatest difference in voltage than the reflection method. This suggests that compared with the reflection method, the transmission method is significantly better at evaluating or detecting changes or variations in the teeth. The reflection method produces small changes, making it hard to recognize or distinguish the state of the tooth.

From the observation, this research demonstrating that greater voltage has better resolution than low frequency due to shorter wavelength; therefore, 25 MHz is a preferable alternative for the range frequency value. Furthermore, compared with the reflection method, the transmission method yields a greater resolution value. The transmission method provides the greatest voltage difference, making it simple to detect changes when a tooth is in an abnormal state. As a result, the transmission method is a much better technique for tomography for a tooth lesion examination.

**Table 6** The difference in the voltage values for the two different methods reflection and transmission methods for the 7- and 25-MHz frequencies

Condition	Frequency	Reflection	Transmission
Enamel	7 MHz	0.150490 V	0.0586480 V
Enamel	25 MHz	0.026944 V	0.0018895 V
Enamel with Air Gap	7 MHz	0.150430 V	0.0545220 V
Enamel with Air Gap	25 MHz	0.026733 V	0.0015054 V
Difference in Voltage Value (Enamel – Enamel with Air Gap)	7 MHz	0.000060 V	0.0041260 V
	25 MHz	0.000211 V	0.0003841 V

## 4.0 CONCLUSION

In conclusion, some modalities have limitations such as discomfort to the patient, distorted images, and radiation exposure. Hence, a conceptual ultrasonic system is chosen to overcome these problems. In this system, a model was designed using the COMSOL software, and different simulations were conducted. Radiographs are routinely used to diagnose approximal tooth surfaces because they cannot be accessed or viewed directly. Although bitewing radiographs are widely recognized as an important tool in the diagnosis of approximal carious lesions, they have several disadvantages owing to their relative insensitivity and reliance on the user for technical performance and interpretation. This proposed system is used to reduce the patient's exposure to ionizing radiation. Furthermore, these alternate approaches for detecting caries are projected to reduce both pollution and the expenses associated with radiographs.

The different simulations were performed (in the COMSOL software) to compare the differences in image reconstruction between when the teeth are in the normal state and when they have anomalies. The system was found capable of detecting and identifying dental irregularities. The simulations for three states (when enamel with the presence of air gap at different position and size) yielded varying results. According to this simulation modeling, when there are anomalies (air gaps) at the tooth, the sensor voltage drops. Because the air gap prevents ultrasonic energy from reaching the receiver, the sensor loss voltage rises as a reaction to it.

Based on a statistical analysis of the voltage readings from ultrasonic receivers, high frequency results in short wavelengths, whereas low frequency results in longer wavelengths. The use of short wavelengths enhances resolution. Furthermore, when compared with the reflection method, the transmission method delivers the biggest volt-age differential. This indicates that the transmission method is substantially better at evaluating or identifying changes or differences in the teeth than the reflection method. The reflection method causes slight changes, making it more difficult to detect or identify the status of the tooth.

The work presented in this manuscript offers opportunities for further studies in some areas. Some of possibilities amendments and improvements in this system is, might broaden the scope of the research in the proposed system. In this case, only the upper front teeth (maxillary central incisor) was used in the research as the conceptual model for the system. In future studies, varying teeth sizes and types can be investigated to validate the frequency range of it. The proposed system simply runs simulations in software; however, it may be extended and enhanced by developing prototype hardware for the ultrasonic tomography system. For example, an unique ultrasonic caries detector is based on the transmission of surface ultrasonic waves and uses a probe that transforms longitudinal vibrations to surface waves when positioned at a precise angle relative to the examined surface. On smooth, flat, or curved surfaces, the latter propagate indefinitely. Sharp angles and interfaces on the surface, far from the ultrasonic probe's contact region, create different echoes.

### Conflicts of Interest

The authors declare that there is no conflict of interest regarding the publication of this paper.

### Acknowledgement

This research is fully supported by Universiti Sains Islam Malaysia, grant number P1-1-12622-UNI-USIM-FKAB.

### References

- [1] J. Jamaludin, M. Zikrillah and Ruzairi. 2013. A Review of Tomography System. *Jurnal Teknologi*. 47-50. Available: <https://oarep.usim.edu.my/jspui/handle/123456789/18295>.
- [2] V. P. Foster. 2021. Carious Lesions: Professional Dental Terminology for the Dental Assistant and Hygienist. [Online]. Available: <https://www.dentalcare.com/en-us/professional-education/ce-courses/ce542/carious-lesions>.
- [3] I. Macleod and H. N. 2008. Cone-beam Computed Tomography (CBCT) in Dental Practice. *Dental Update*. 9(35): 590-598. Available: <https://www.magonlinelibrary.com/doi/abs/10.12968/denu.2008.35.9.590?journalCode=denu>.
- [4] P. M. Jørgensen and W. A. 2012. Patient Discomfort in Bitewing Examination with Film and Four Digital Receptors. *Dentomaxillofacial Radiology*. 4(41): 323-327. Available: <https://www.birpublications.org/doi/full/10.1259/dmfr/73402308>.
- [5] N. Shah, B. N. and L. A. 2014. Recent Advances in Imaging Technologies in Dentistry. *World Journal of Radiology*. 10(6): 794. Available: <https://www.ncbi.nlm.nih.gov/pmc/articles/PMC4209425/>.
- [6] Longbottom and A. F. Z. Christopher. 2019. *Detection and Assessment of Dental Caries*. London, UK: Springer. 47-50. Available: <https://link.springer.com/book/10.1007/978-3-030-16967-1>.
- [7] I. M. N. Heath. 2008. Cone Beam Computed Tomography (CBCT) in Dental Practice. *Dental and Maxillofacial Radiology*. 590-597. Available: <https://www.magonlinelibrary.com/doi/abs/10.12968/denu.2008.35.9.590?journalCode=denu>.
- [8] A. S. Y. Yasushi Shimada. 2015. Application of Optical Coherence Tomography (OCT) for Diagnosis of Caries, Cracks and defects of Restoration. *Curr Oral Health*. 73-80. Available: <https://link.springer.com/article/10.1007/s40496-015-0045-z>.
- [9] S. Aumann, D. S. F. J. and M. F. 2019. Optical Coherence Tomography (OCT): Principle and Technical Realization. *High Resolution Imaging in Microscopy and Ophthalmology*. 59-85. Available: [https://link.springer.com/chapter/10.1007/978-3-030-16638-0\\_3](https://link.springer.com/chapter/10.1007/978-3-030-16638-0_3).
- [10] Al-Khuwaitem and R. W. 2019. The Use of Optical Coherence Tomography as a Diagnostic Tool for Dental Caries. Doctoral Dissertation. UCL (University College London). Available: <https://discovery.ucl.ac.uk/id/eprint/10084080/>.
- [11] Niraj, L. K., Patthi, S. B., G. R. A., I. D. Ali and .. & P. M. K. 2016. MRI in Dentistry-a Future Towards Radiation Free Imaging-systematic Review. *Journal of Clinical and Diagnostic Research: JCDR*. 10(10). Available: <https://www.ncbi.nlm.nih.gov/pmc/articles/PMC5121829/>.
- [12] Magnetic Resonance Imaging (MRI). 2021. National Institute of Biomedical Imaging and Bioengineering, [Online]. Available: <https://www.nibib.nih.gov/science-education/science-topics/magnetic-resonance-imaging-mri>. [Accessed 16 November 2021].
- [13] Husniye Demirturk Kocasarac; Christos Angelopoulos. 2018. Ultrasound in Dentistry Toward a Future of Radiation-Free Imaging. *Dental Clinics*. 3(62): 481-489. Available: [https://www.dental.theclinics.com/article/S0011-8532\(18\)30022-3/fulltext](https://www.dental.theclinics.com/article/S0011-8532(18)30022-3/fulltext).
- [14] F. Caglayan and B. I. S. 2018. The Intraoral Ultrasonography in Dentistry. *Nigerian Journal of Clinical Practice*. 2(21): 125-133. Available: <https://www.ajol.info/index.php/njcp/article/view/167428>.
- [15] S. Sharma, R. D. S. M. and M. M. 2014. Ultrasound as a Diagnostic Boon in Dentistry-A Review. *International Journal of Scientific Study*. 2(2): 70-76.
- [16] S. Braun, & H. J. S. 2000. Ultrasound Imaging of Condylar Motion: A Preliminary Report. *The Angle Orthodontist*. 5(70): 383-386. Available:

- <https://meridian.allenpress.com/angleorthodontist/article/70/5/383/57542/Ultrasound-Imaging-of-Condylar-Motion-A>.
- [17] P. Pattnaik, P. S. K., K. S. K. and &. D. P. Das. 2012. Studies of Lead Free Piezo-Electric Materials Based Ultrasonic MEMS Model for Bio Sensor. *Proceeding of COMSOL Conference*.
- [18] T. Li, C. Y. &. M. J. 2009. Development of a Miniaturized Piezoelectric Ultrasonic Transducer. *IEEE Transactions on Ultrasonics, Ferroelectrics, and Frequency Control*. 3(56): 649-659. Available: <https://ieeexplore.ieee.org/abstract/document/4816072/>.
- [19] S. Katzir. 2006. The Discovery of the Piezoelectric Effect. *The Beginnings of Piezoelectricity*. 15-64. Available: [https://link.springer.com/chapter/10.1007/978-1-4020-4670-4\\_2](https://link.springer.com/chapter/10.1007/978-1-4020-4670-4_2).
- [20] Wang, H. C., Fleming, S., Lee, Y. C., Swain, M., Law, S., & Xue, J. 2011. Laser Ultrasonic Evaluation of Human Dental Enamel During Remineralization Treatment. *Biomedical Optics Express*. 11(2): 345-355. Available: <https://opg.optica.org/boe/viewmedia.cfm?uri=boe-2-2-345&html=true>.
- [21] T. D. Case. 1998. Ultrasound Physics and Instrumentation. *Surgical Clinics of North America*. 2(78): 197-217. Available: [https://doi.org/10.1016/S0039-6109\(05\)70309-1](https://doi.org/10.1016/S0039-6109(05)70309-1).